

INTEGRATED ELECTRO-THERMAL PROBE

Ronald M. Reano, Kyoung Yang, John F. Whitaker, and Linda P. B. Katehi

Radiation Laboratory and Center for Ultrafast Optical Science, Department of Electrical Engineering and Computer Science, University of Michigan, Ann Arbor, MI 48109, USA

Abstract — A method to simultaneously measure electric and thermal fields with a single probe is presented. The probe material is gallium arsenide with the Pockels effect employed to measure electric fields and the effect of photon absorption due to bandtail states used to determine temperature. Measured optical power versus temperature is inversely related and is shown to agree with theory. Experimental results demonstrate a sensitivity of $0.31 \mu\text{W}/^\circ\text{C}$ at 25°C and an accuracy of $\pm 0.5^\circ\text{C}$ between 20°C and 60°C . The magnitude of the electric field is obtained with a normalized standard deviation of 1.3%. The technique is applied to the combined electro-thermal examination of an MMIC in a quasi-optical power-combining array and the calibration of electric field data that was corrupted by temperature dependent effects inherent to the electro-optic probe.

I. INTRODUCTION

The electro-thermal behavior of active microwave and millimeter wave circuits has received growing attention in recent years [1]-[3]. The thermal characteristics become especially important in active antenna arrays and quasi-optical power combining structures where a multitude of biased MMICs are in close proximity. The generation of heat in such configurations mandates a strong consideration of heat dissipation in the overall design [4]-[5].

Several methods have been developed to characterize and diagnose the behavior of such circuits. To examine the electrical behavior, optical techniques such as those that use electro-optic probes for the non-contact field-mapping of electric fields have been employed [6]-[7]. Separate methods exist for observing thermal effects including the use of thermal cameras, IR microscopes, thermocouples, and thermistors.

A major factor that has yet to be considered when applying electro-optic field mapping techniques to the characterization of active microwave circuits is the temperature dependence of the probe itself. The electro-optic coefficients that govern the response of the probe to RF fields are known to vary with temperature [8]. Additionally, in III-V semiconductor-based probes, the temperature dependence of the optical absorption edge is significant. The sensitivity of the absorption edge to temperature has been used, for example, to monitor the

temperature in indium-phosphide-based semiconductor substrates where knowledge of the epitaxial growth temperature is critical [9].

This paper addresses the temperature dependent effects associated with GaAs electro-optic probes. From this study, it is shown that both electric and thermal fields can be measured simultaneously. This allows for the combined electro-thermal examination of active microwave and millimeter-wave circuits with a single probe and the ability to calibrate electric field data that is corrupted when the probe is placed in areas where temperature variations are present.

II. THEORY

The physical mechanisms employed to measure temperature are the temperature dependence of the energy bandgap in intrinsic semiconductors and its effect on the absorption of optical power. A well known equation describing this phenomena has been established by Varshini [10]

$$E_g(T) = E_g(0) - \frac{\gamma T^2}{T + \beta} \quad (1)$$

where γ and β are material-specific empirical constants, $E_g(T)$ is the bandgap energy at temperature T , and $E_g(0)$ is the bandgap energy at zero kelvin. For photon energies in the bandgap and near the band-edge, the absorption coefficient, α , has been found to decay exponentially with decreasing photon energy, $h\nu$, due to the presence of bandtail states. The dependence on photon energy is shown to follow [11]

$$\alpha = A \exp[(h\nu - x_o) / y_o] \quad (2)$$

where A , x_o , and y_o are constant curve fitting parameters at 300 K. For GaAs at room temperature ± 70 K, the bandgap and absorption coefficient variation with temperature can be linearized to within 5%. Linearizing equation (1) and (2) about a nominal temperature, T_o , and photon energy $(h\nu)_o$ and noting that

$$\frac{\partial \alpha}{\partial (h\nu)} = \xi \frac{\partial \alpha}{\partial E_g} \quad (3)$$

where ξ is a constant on the order of one for the temperature range of interest, the flow of optical power, P , through the semiconductor is found to obey the following temperature dependence

$$\frac{1}{P} \propto 1 + \kappa T \quad (4)$$

where κ is a constant that depends on the dimension of the semiconductor in the direction of propagation. Therefore, by monitoring the absorption response of an optical beam that is directed to propagate through a section of semiconducting material, the change in temperature can be inferred in a manner that is linear with the inverse of optical power.

To simultaneously measure electric fields, the semiconductor must also be electro-optic. Due to the Pockels effect, an optical beam propagating through an electro-optic material exhibits a change in polarization-state when the material is in the presence of an externally applied electric field. The change in polarization-state can be made to result in an amplitude modulation of the optical beam that is proportional to the intensity of the applied electric field. The optical transmission, T , through an electro-optic modulator set up for 50% transmission, is given by [8]

$$T = \sin^2 \left[\frac{1}{2} \left(\frac{\pi}{2} + \pi \frac{E_{rf} d}{V_{\pi}} \sin(\omega_{rf} t) \right) \right] \quad (5)$$

where E_{rf} is the RF electric field magnitude in the probe, d is the probe thickness in the direction of propagation of the optical beam, ω_{rf} is the RF frequency, t is time, and V_{π} is the half-wave voltage of the electro-optic material. For $E_{rf} d \ll V_{\pi}$, the intensity modulation is linear with applied RF electric field.

III. IMPLEMENTATION

The experimental setup is shown in Figure 1. The probe material is GaAs with a normal-surface area of $500 \mu\text{m} \times 500 \mu\text{m}$ and a vertical thickness of $200 \mu\text{m}$. A Ti:Sapphire laser tuned to 895 nm is used to generate a linearly polarized sampling beam that is coupled to the probe via a section of single-mode optical fiber and a graded-index lens [12]. Appropriate phase retarders are placed to configure a 50% transmission intensity modulator for electric field measurements.

To alleviate the need for a fast photodetector, and to provide a method by which the phase of a signal may also be easily sensed, the device under test is fed via an RF synthesizer configured for harmonic mixing in order to down-convert the sampled electric fields to IF frequencies.

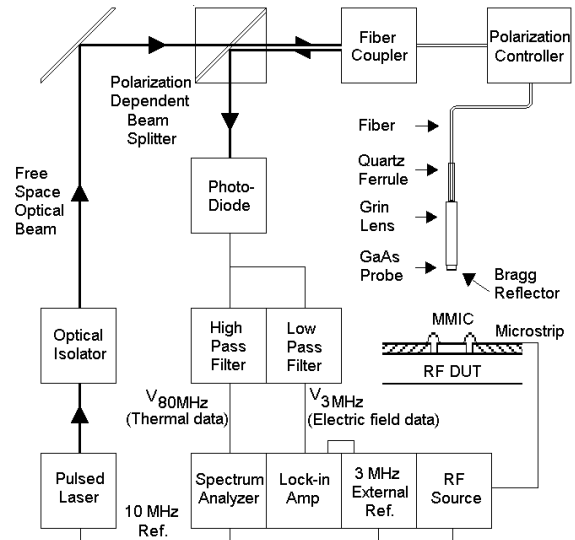


Fig. 1. The experimental setup with a typical RF device-under-test (DUT). In the figure, the DUT is an MMIC with a microstrip feed.

This is accomplished by mode locking the laser to produce a train of 80 fs pulses at a pulse repetition rate of 80 MHz and setting the RF source frequency to an integer multiple of the pulse repetition rate, plus an offset that corresponds to the IF frequency. An IF frequency of 3 MHz is used and was selected based on a tradeoff consideration between signal-to-noise degradation due to $1/f$ noise at lower IF frequencies and the loss of sensitivity incurred by selecting higher IF frequencies [6]. Since the 80-MHz component is not modulated coherently, its amplitude does not change as it passes through the electro-optic crystal.

A photodiode functions as an envelope detector that transforms the 3 MHz modulation and the 80 MHz pulse repetition component to electrical signals for detection. The 3-MHz signal, denoted $V_{3\text{MHz}}$, is the modulation signal that provides the electric field information and the 80-MHz signal, denoted $V_{80\text{MHz}}$, is the spectral component that is monitored for temperature measurements. A high-pass filter that filters as an open-circuit couples the 80-MHz pulse-repetition component to a spectrum analyzer while the 3-MHz modulation signal is coupled to a lock-in amplifier with a low pass filter that filters as an open-circuit for the 80-MHz signal. Such an arrangement allows for the simultaneous measurement of thermal and electric fields.

IV. CHARACTERIZATION

To characterize the thermal properties of the probe, it was mounted in still air approximately four inches above a hotplate. A precision thermistor with a tolerance of $\pm 0.2^\circ\text{C}$ was positioned adjacent to the probe to monitor the

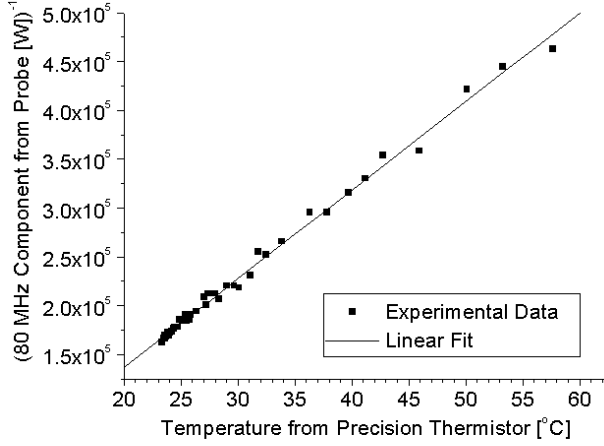


Fig. 2. The temperature response of the GaAs probe.

temperature variations of the ambient air as the hot plate was turned on and off. Absorption data from the probe and temperature data from the thermistor were collected over a fifty minute period as the temperature was varied between 20°C and 60°C. The results are shown in Figure 2 and agree with the theory as described in equation (4).

The temperature accuracy and sensitivity of the probe are determined from a linear regression analysis of the data shown in Fig. 2. The accuracy, calculated from the standard deviation of the data set composed of the absolute value of the deviations from the linear fit, is calculated to be $\pm 0.5^\circ\text{C}$. Using the thermistor resistance versus temperature characteristic and the observed relationship between the measured optical power and the thermistor resistance, the sensitivity is calculated to be equal to $0.31 \mu\text{W}/^\circ\text{C}$ at 25°C .

V. APPLICATIONS

To demonstrate the usefulness of the electro-thermal probe, the thermal and electric fields of a single MMIC cell within an X-band quasi-optical power-combining array was examined. A horn antenna fed an RF signal to an array of patch antennas, which coupled power to a set of amplifying MMICs via microstrip line. The output of each MMIC was re-radiated via an array of patch antennas allowing free-space power-combining to be accomplished.

The probe was mounted near the output of the MMIC and less than 0.5 mm above the microstrip substrate. For comparison purposes, a power meter was mounted in the far-field of the array in order to independently monitor its output performance. To isolate the MMIC under test, the input and output patch antennas for all the other MMICs were covered with copper tape. The bias and RF for the array was switched on at time zero. Figure 3 clearly shows that there is a substantial difference between the behavior

of the measured electric field data obtained from the probe and the measured power from the independent power meter. The explanation for the discrepancy is shown in Figure 4 as the absorption data from the probe is seen to decrease with time along with the electric field data. The change in the absorption signal is consistent with the expected increase in temperature in the vicinity of the biased MMIC due to the dissipation of heat.

Calibration of the temperature effects of the probe on the electric-field measurements is possible since the absorption signal is linearly proportional to the electric-field signal. Knowledge of the deviation of the absorption signal with time, $\Delta V_{80\text{MHz}}$, allows for the compensation of the modulation signal for temperature effects according to

$$V'_{3\text{MHz}} = \left(\frac{dV_{3\text{MHz}}}{dV_{80\text{MHz}}} \right) \Delta V_{80\text{MHz}} + V_{3\text{MHz}} \quad (6)$$

where the primed notation denotes temperature-calibrated data. The results of this calibration method are shown in Figure 5. The calibrated electric-field data is now in excellent agreement with the independent power-meter measurements. The calculated standard deviation is 1.3%.

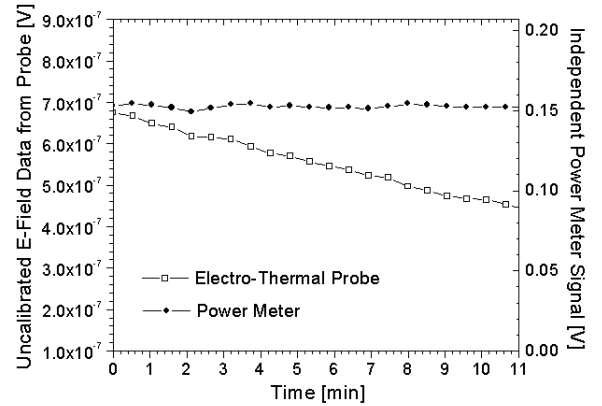


Fig. 3. Probe and power meter measurements of MMIC.

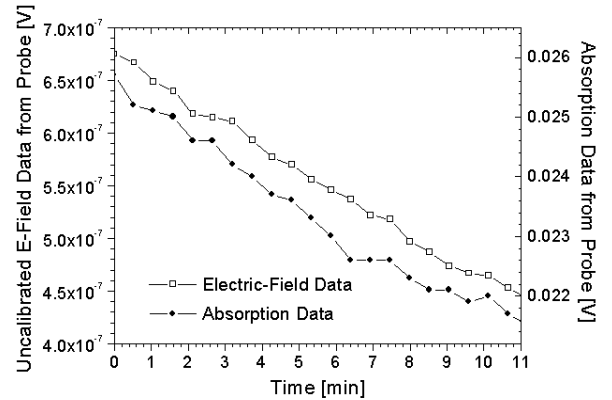


Fig. 4. Probe-only measurements of MMIC.

Figure 6 illustrates the results from the simultaneous data collected from the probe. Knowledge of the initial room temperature, the optical-power/temperature relationship, and the deviation of the 80-MHz component with time allow for the scaling of the 80-MHz component to degrees celsius. The region neighboring the output of the MMIC is seen to increase by 7°C in 11 minutes.

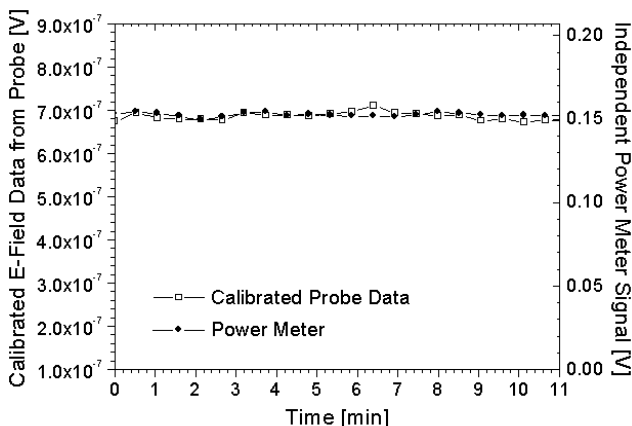


Fig. 5. Temperature-calibrated electric field data.

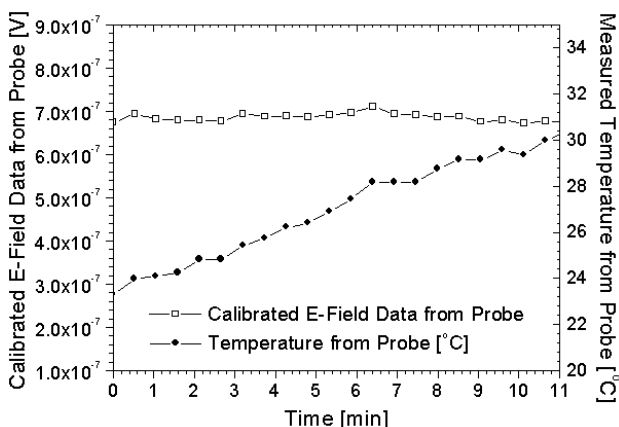


Fig. 6. Simultaneous electric-field and temperature measurements of MMIC.

VI. CONCLUSION

An integrated electro-thermal probe capable of simultaneously measuring thermal and electric fields is presented. Experimental observations of the response of the probe to thermal and electric fields is shown to be consistent with theoretical expectations. This novel measurement technique can provide new and fundamental insight into the combined electro-thermal behavior of complex active microwave and millimeter-wave structures and allows for the calibration of electric field data that is corrupted when the probe is used in regions where temperature gradients exist.

ACKNOWLEDGEMENTS

The authors wish to thank Amir Mortazawi of North Carolina State University for the use of the quasi-optical power-combining array. This work was supported by the ARO Spatial and Quasi-Optical Power Combining MURI (contract DAAG 55-97-0132).

REFERENCES

- [1] W. Batty, A. J. Panks, R. G. Johnson and C. M. Snowden, "Electro-thermal modeling and measurement for spatial power combining at millimeter wavelengths," *IEEE Trans. Microwave Theory and Tech.*, vol. MTT-47, no. 12, pp. 2574-2585, Dec. 1999.
- [2] H. M. Gutierrez, C. E. Christoffersen, and M. B. Steer, "An integrated environment for the simulation of electrical, thermal and electromagnetic interactions in high-performance integrated circuits," *IEEE 8th Topical Meeting on Electrical Performance of Electronic Packaging*, pp. 217-20, Oct. 1999.
- [3] R. G. Johnson, C. M. Snowden and R. D. Pollard, "A physics-based electro-thermal model for microwave and millimeter wave HEMTs," *1997 IEEE MTT-S Int. Microwave Symp. Dig.*, vol. 3, pp. 1485-1488, June 1997.
- [4] N. S. Cheng, P. Jia, D. B. Rensch and R. A. York, "A 120-W X-band spatially combined solid-state amplifier," *IEEE Trans. Microwave Theory and Tech.*, vol. MTT-47, no. 12, pp. 2557-2561, Dec. 1999.
- [5] J. Hubert, L. Mirth, S. Ortiz and A. Mortazawi, "A 4 Watt Ka-band quasi-optical amplifier," *1999 IEEE MTT-S Int. Microwave Symp. Dig.*, vol. 2, pp. 551-554, June 1999.
- [6] K. Yang, L. P. B. Katehi and J. F. Whitaker, "Electro-optic field mapping system utilizing external gallium arsenide probes," *Applied Physics Letters*, vol. 77, no. 4, pp. 486-488, July 2000.
- [7] S. Wakana, T. Ohara, M. Abe, E. Yamazaki, M. Kishi, and M. Tsuchiya, "Novel electromagnetic field probe using electro/magneto-optical crystals mounted on optical-fiber facets for microwave circuit diagnostics," *2000 IEEE MTT-S Int. Microwave Symp. Dig.*, vol. 3, pp. 1615-1618, June 2000.
- [8] A. Yariv and P. Yeh, *Optical Waves in Crystals*, New York: John Wiley & Sons, Inc., 1984.
- [9] M. Beaudoin, S. R. Johnson, A. J. G. DeVries, A. Mohades-Kassai, T. Tiedje, R. J. Shul, S. J. Pearton, F. Ren, C. S. Wu, "Temperature dependence of the optical absorption edge in indium phosphide," *Compound Semiconductor Electronics and Photonics – Symposium*, pp. 367-72, Apr. 1996.
- [10] C. D. Thurmond, "The standard thermodynamic functions for the formation of electrons and holes in Ge, Si, GaAs and GaP," *J. Electrochem. Soc.*, Vol. 122, No. 8, pp. 1133-1141, Aug. 1975.
- [11] H. C. Casey, D. D. Sell, and K. W. Wecht, "Concentration dependence of the absorption coefficient for n- and p-type GaAs between 1.3 and 1.6 eV," *J. Appl. Phys.*, Vol. 46, No. 1, pp. 250-257, Jan. 1975.
- [12] K. Yang, L. P. B. Katehi, and J. F. Whitaker, "Electric-field mapping system using an optical-fiber-based electro-optic probe," submitted to *IEEE Microwave Guided Wave Lett.*